Table 8 | Continued

Disease	Genetic defect; presumed pathogenesis	Inheritance	Functional defect	Associated features	OMIM number
13. C1 inhibitor deficiency	Mutation in *SERPING1*: regulation of kinins and complement activation	AD	Spontaneous activation of the complement pathway with consumption of C4/C2 Spontaneous activation of the contact system with generation of bradykinin from high molecular weight kininogen	Hereditary angioedema	138470
14. Factor B[a]	Mutation in *CFB*: activation of the alternative pathway	AD	Gain-of-function mutation with increased spontaneous AH50	aHUS	138470
15. Factor D deficiency	Mutation in *CFD*: regulation of the alternative complement pathway	AR	Absent AH50 hemolytic activity	Neisserial infections	134350
16. Properdin deficiency	Mutation in *CFP*: regulation of the alternative complement pathway	XL	Absent AH50 hemolytic activity	Neisserial infections	312060
17. Factor I deficiency	Mutation in *CFI*: regulation of the alternative complement pathway	AR	Spontaneous activation of the alternative complement pathway with consumption of C3	Infections, Neisserial infections, aHUS, preeclampsia, membranoproliferative glomerulonephritis (MPGN)	610984
18. Factor H deficiency	Mutation in *CFH*: regulation of the alternative complement pathway	AR	Spontaneous activation of the alternative complement pathway with consumption of C3	Infections, Neisserial infections, aHUS, preeclampsia, membranoproliferative glomerulonephritis (MPGN)	609814
19. Factor H-related protein deficiencies	Mutation in *CFHR1-5*: bind C3b	AR	Normal CH50, AH50, autoantibodies to Factor H	aHUS	235400
20. Thrombomodulin[a]	Mutation in *THBD*: regulates complement and coagulant activation	AD	Normal CH50, AH50	aHUS	188040
21. MASP1 deficiency	Mutation in *MASP1*: cleaves C2 and activates MASP2	AR	Deficient activation of the lectin activation pathway, cell migration	Infections, 3MC syndrome	600521
22. MASP2 deficiency[a]	*MASP2*: cleavage of C2 and C4	AR	Deficient activation of the lectin activation pathway	Pyogenic infections; inflammatory lung disease, autoimmunity	605102
23. 3MC syndrome COLEC11 deficiency[a]	Mutation in *COLEC11*: binds MASP1, MASP3	AR	Loss of neural crest cell migration signals	A developmental syndrome of facial dysmorphism, cleft lip and/or palate, craniosynostosis, learning disability, and genital, limb, and vesicorenal anomalies (3MC syndrome)	612502

(Continued)

Table 8 | Continued

Disease	Genetic defect; presumed pathogenesis	Inheritance	Functional defect	Associated features	OMIM number
24. Complement receptor 2 (CR2) deficiency[a]	Mutation in CD21	AR	See CD21 deficiency in **Table 3**		120650
25. Complement receptor 3 (CR3) deficiency	Mutation in ITGB2	AR	See LAD1 in **Table 5**		116920
Membrane cofactor protein (CD46) deficiency	Mutation in CD46: dissociates C3b and C4b	AD	Inhibitor of complement alternate pathway, decreased C3b binding	aHUS, infections, preeclampsia	120920
Membrane Attack Complex inhibitor (CD59) deficiency[a]	Mutation in CD59: regulates the membrane attack complex formation	AR	Erythrocytes highly susceptible to complement-mediated lysis	Hemolytic anemia, polyneuropathy	107271
Ficolin 3 deficiency[a]	Mutation in FCN3: activates the classical complement pathway	AR	Absence of complement activation by the Ficolin 3 pathway	Respiratory infections, abscesses	604973

XL, X-linked inheritance; AR, autosomal recessive inheritance; AD, autosomal dominant inheritance; MAC, membrane attack complex; SLE, systemic lupus erythematosus; MBP, mannose-binding protein; MASP2, MBP-associated serine protease 2.

[a]Ten or fewer unrelated cases reported in the literature.

New entities added to **Table 8** demonstrate the important role of complement regulators in a group of well-described inflammatory disorders. In particular, we have added mutations in membrane bound as well as surface attached soluble complement regulatory proteins recognized in hemolytic–uremic syndrome, age-related macular degeneration, and preeclampsia. The connecting theme of these otherwise unrelated clinical events is excessive activation or insufficient regulation of C3; these events lead to recruitment of leukocytes and permit secretion of inflammatory and anti-angiogenic mediators that disrupt the vascular bed of the target organ. Alterations in the genes for Factor B (CFB), Factor I (CFI), Factor H (CFH), and CD46 act as susceptibility genes rather than disease causing mutations. Population studies reveal no detectable increase in infections in MBP (also known at mannose-binding lectin – MBL) deficient adults. The 3MC syndrome, a developmental syndrome, has been variously called Carnevale, Mingarelli, Malpuech, and Michels syndrome.

Table 9 | Phenocopies of PID.

Disease	Genetic defect/ presumed pathogenesis	Circulating T cells	Circulating B cells	Serum Ig	Associated features/ similar PID
Associated with somatic mutations					
(a) Autoimmune lymphoproliferative syndrome (ALPS–SFAS)	Somatic mutation in TNFRSF6	Increased CD4⁻ CD8⁻ double negative (DN) T alpha/beta cells	Normal, but increased number of CD5⁺ B cells	Normal or increased	Splenomegaly, lymphadenopathy, autoimmune cytopenias Defective lymphocyte apoptosis/ALPS–FAS (=ALPS type Im)
(b) RAS-associated autoimmune leukoproliferative disease (RALD)	Somatic mutation in KRAS (gain-of-function)	Normal	B cell lymphocytosis	Normal or increased	Splenomegaly, lymphadenopathy, autoimmune cytopenias, granulocytosis, monocytosis/ALPS-like

(Continued)

— 101 —

Table 9 | Continued

Disease	Genetic defect/ presumed pathogenesis	Circulating T cells	Circulating B cells	Serum Ig	Associated features/ similar PID
(c) RAS-associated autoimmune leukoproliferative disease (RALD)	Somatic mutation in *NRAS* (gain-of-function)	Increased CD4⁻ CD8⁻ double negative (DN) T alpha/beta cells	Lymphocytosis		Splenomegaly, lymphadenopathy, autoantibodies/*ALPS-like*
Associated with autoantibodies					
(a) Chronic mucocutaneous candidiasis (isolated or with APECED syndrome)	Germline mutation in *AIRE* AutoAb to IL-17 and/or IL-22	Normal	Normal	Normal	Endocrinopathy, chronic mucocutaneous candidiasis/*CMC*
(b) Adult-onset immunodeficiency	AutoAb to IFN gamma	Decreased naive T cells	Normal	Normal	Mycobacterial, fungal, *Salmonella* VZV infections/*MSMD, or CID*
(c) Recurrent skin infection	AutoAb to IL-6	Normal	Normal	Normal	Staphylococcal infections/*STAT3 deficiency*
(d) Pulmonary alveolar proteinosis	AutoAb to GM-CSF	Normal	Normal	Normal	Pulmonary alveolar proteinosis, cryptococcal meningitis/*CSF2RA deficiency*
(e) Acquired angioedema	AutoAb to CI inhibitor	Normal	Normal	Normal	Angioedema/*C1 INH deficiency* (hereditary angioedema)

The rapid advances in gene identification technology, including the widespread use of whole exome and whole genome sequencing, has meant that the ability to identify gene defects in affected families and even single individuals with inherited diseases has grown enormously. In this report, over 30 new gene defects have been added that were identified since the previous classification in November, 2011. These defects can be found in all major groups of PIDs included in this report. In many cases, the mutations are not necessarily in genes formally implicated in immune cell function but are genes involved in essential cell processes. The more detailed analysis and functional consequences of such defects as illustrated by these PIDs will increase our understanding of the interplay between different cellular processes in the development and function of the immune system.

Among the newly identified, gene defects are many that are to date particular to a single pedigree or individual; such defects may prove exceedingly rare, or indeed may not necessarily be found to recur in other individuals. We have marked conditions for which there are 10 or fewer reported individuals with an asterisk, although historically, following the description of the first few cases, additional individuals with a similar PID phenotype and genotype have often been recognized. It is likely that we will uncover many more "personal" or very rare gene defects over time

and that the spectrum of PIDs will become increasingly diverse and complex, due to contributions of both environmental exposures and genetic modifiers to each affected individual. The value of this report therefore to capture and catalog the full spectrum at any one time point becomes increasingly important.

The goal of the IUIS Expert Committee on PIDs is to increase awareness, facilitate recognition, and promote optimal treatment for patients with PIDs. In addition to the current report and previous "classification table" publications, the committee has also produced a "Phenotypic Approach for IUIS PID Classification and Diagnosis: Guidelines for Clinicians at the Bedside," which aims to lead physicians to particular groups of PIDs starting from clinical features and combining routine immunological investigations. Together, these contributions will hopefully allow a practical clinical framework for PID diagnosis. The committee also aims to establish a classification of PIDs based on other aspects and will work on publishing further guidelines in due course.

Familial Mediterranean Fever
Genotype-Phenotype Correlations in Japanese Patients

Kiyoshi Migita, MD, PhD, Kazunaga Agematsu, MD, PhD, Masahide Yazaki, MD, PhD,
Fumiaki Nonaka, MD, PhD, Akinori Nakamura, MD, PhD, Tomoko Toma, MD, PhD,
Dai Kishida, MD, PhD, Ritei Uehara, MD, PhD, Yoshikazu Nakamura, MD, PhD, Yuka Jiuchi, PhD,
Junya Masumoto, MD, PhD, Hiroshi Furukawa, MD, PhD, Hiroaki Ida, MD, PhD, Chihiro Terai, MD, PhD,
Yoshikazu Nakashima, MD, PhD, Atsushi Kawakami, MD, PhD, Tadashi Nakamura, MD, PhD,
Katsumi Eguchi, MD, PhD, Michio Yasunami, MD, PhD, and Akihiro Yachie, MD, PhD

Abstract: Familial Mediterranean fever (FMF) is an autoinflammatory disease caused by MEditerranean FeVer gene (MEFV) mutations. In Japan, patients with FMF have been previously reported, including a mild or incomplete form. Several factors are presumed to contribute to the variable penetrance and to the phenotypic variability of FMF. We conducted the current study to investigate the correlation of variable clinical presentations and MEFV genotypic distributions in Japanese FMF patients.

We analyzed demographic, clinical, and genetic data for 311 FMF patients enrolled in the study. Clinically, we classified FMF into 2 phenotypes: 1) the "typical" form of FMF, and 2) the "atypical" form of FMF according to the Tel Hashomer criteria. Patients with the typical FMF phenotype had a higher frequency of febrile episodes, a shorter duration of febrile attacks, more frequent thoracic pain, abdominal pain, a family history of FMF, and MEFV exon 10 mutations. Conversely, patients with the atypical FMF phenotype had a lower frequency of fever episodes and more frequent arthritis in atypical distribution, myalgia, and MEFV exon 3 mutations. Multivariate analysis showed that the variable associated with typical FMF presentation was the presence of MEFV exon 10 mutations. Typical FMF phenotype frequencies were decreased in patients carrying 2 or a single low-penetrance mutations compared with those carrying 2 or a single high-penetrance mutations (M694I), with an opposite trend for the atypical FMF phenotype. In addition, patients having more than 2 MEFV mutations had a younger disease onset and a higher prevalence of thoracic pain than those carrying a single or no mutations. Thus, MEFV exon 10 mutations are associated with the more typical

FMF phenotype. In contrast, more than half of the Japanese FMF patients without MEFV exon 10 mutations presented with an atypical FMF phenotype, indicating that Japanese FMF patients tend to be divided into 2 phenotypes by a variation of MEFV mutations.

(*Medicine* 2014;93: 158–164)

Abbreviations: CI = confidence interval, FMF = familial Mediterranean fever, IL-1β = interleukin 1 beta, OR = odds ratio.

INTRODUCTION

Familial Mediterranean fever (FMF) is an autosomal recessive autoinflammatory disease caused by MEditerranean FeVer gene (MEFV) mutations on chromosome 16,[1,7] and characterized by periodic fever and serositis.[24] The disease occurs most commonly in populations of eastern Mediterranean descent. However, patients of various ethnic origins are well documented, including several Japanese individuals.[29,33] FMF can be classified as "typical" and "atypical" types based on clinical findings and genetic screening.[13,20] As indicated in the Tel Hashomer criteria,[13] a typical FMF attack is defined as episodes lasting 12 hours to 3 days with fever accompanied by peritonitis, pleuritis, or monoarthritis of hip, knee, or ankle. In contrast, an incomplete attack differs from the definition of a typical attack in the following features: temperature of less than 38°C; attack duration longer or shorter than specified periods (12 hours to 3 days), but not shorter than 6 hours or longer than a week; localized abdominal signs; or atypical distribution of arthritis.[13] In addition, Ryan et al[20] reported patients with symptoms of the syndrome of periodic fever, aphthous stomatitis, pharyngitis, and cervical adenitis in atypical FMF. Although MEFV genotyping has enabled FMF to be confirmed in some cases, the diagnosis remains predominantly clinical since genotyping has shown that the disease is characterized by variable manifestations.[19,28]

To date, over 200 disease-associated mutations have been identified in MEFV, with the majority of mutations being missense changes and more than half clustering in exons 2 and 10.[31] The presence of mutations on both MEFV alleles establishes a diagnosis of FMF, but in many cases only a single mutation or no mutation can be identified,[12,14] resulting in a diagnostic dilemma. Additionally, some patients carrying MEFV mutations either as heterozygotes, compound heterozygotes, or complex alleles present with various atypical FMF clinical manifestations.[17] In contrast to typical FMF cases in endemic areas, some FMF patients lack a classic clinical presentation, and a diagnosis is therefore difficult in populations where the disease is rare.[3] Another problem is that the penetrance of a disease-causing mutation varies by MEFV mutations. Manifestation of FMF symptoms is mainly attributed to the high

frequency of low-penetrance mutations (E148Q, V726A, etc) and the low frequency of high-penetrance mutations (M694V, M694I, etc).[8] The low-penetrance pyrin mutation E148Q is found frequently in east Asia. The V726A mutation remains practically totally silent and nonpenetrant in Ashkenazi Jews.[9]

Although our knowledge of FMF is expanding rapidly,[22] it remains very limited in Japan because of the rarity and phenotypic variability of Japanese FMF.[16] To avoid the delayed disease diagnosis that might be associated with this, we conducted a nationwide survey and laboratory testing for the genetic diagnosis of FMF patients. We aimed to provide clear and comprehensive demographic data regarding Japanese patients with typical/incomplete FMF, and to analyze the impact of genetic factors on the disease phenotype in a large population of Japanese FMF patients.

METHODS

Patient Enrollment

A nationwide survey of FMF was conducted in cooperation with the Japan Research Committee on the Epidemiology of Intractable Diseases in 2009.[16] Patients were diagnosed clinically according to the Tel Hashomer diagnostic criteria.[13] Epidemiologic data (including sex, consanguinity of parents, familial history, and age of onset of inflammation signs) and main clinical data (including fever; thoracic, abdominal, articular, and cutaneous signs; duration and frequency of episodes; presence of amyloidosis; and response to colchicine) were recorded by the doctor in charge using a standard form. A diagnosis of FMF was made if the patient had 1 or more major criteria, or 2 or more minor criteria of the Tel Hashomer criteria.[13] On the basis of the Tel Hashomer criteria, we divided the study subjects into 2 groups, typical FMF and atypical FMF. Typical FMF patients had the typical episode of peritonitis, pleuritis, monoarthritis, or fever alone as specified in the Tel Hashomer criteria. Atypical FMF patients had an "incomplete" attack. An attack was considered incomplete if it differed from the definition of a typical attack in only 1 or 2 of the following features: temperature less than 38°C; attack duration longer or shorter than specified periods (12 hours to 3 days), but not shorter than 6 hours or longer than a week; no signs of peritonitis during an abdominal attack, or signs were localized; atypical distribution of arthritis. The present study was approved by the ethical committees of Nagasaki Medical Center (No. 21015, 2009).

Mutational Analysis

Blood samples (2 mL) were collected from all subjects. Genomic DNA was extracted from whole blood by means of the Promega Wizard Genomic DNA Purification Kit (Promega, Madison, WI). Mutation analysis was performed by direct DNA sequencing. Polymerase chain reaction (PCR) was performed using the forward and reverse primers for each exon of the MEFV gene as described previously.[27] PCR products were purified with the ExoSAP-IT (GE Healthcare Japan, Tokyo, Japan) and sequenced directly, using specific primers and BigDye Terminator v1.1 (Applied Biosystems, Tokyo, Japan). MEFV genetic analysis was approved by the Ethics Committee of Nagasaki Medical Center (No. 21003, 2009).

Statistical Analyses

We used SPSS software (SPSS Inc, Chicago, IL) to analyze the data. Results were expressed as the mean ± standard deviation for continuous variables. For quantitative data, analysis was performed using a Mann–Whitney U rank-sum test to compare 2 independent groups. Comparisons for categorical variables

were evaluated using the chi-square test (or the Fisher exact test when appropriate).

We used logistic regression models to detect variables that affect disease phenotype. All possible variables were initially evaluated by univariate analysis, then suitable candidates for multivariate analysis were chosen that had a p value < 0.1 plus additional variables of known biological importance. The forward likelihood logistic regression approach was used to define variables that may affect the FMF phenotype. A p value < 0.05 was accepted as significant.

RESULTS

Demographic Features

A total of 311 patients were enrolled in this study: 185 patients lived in East Japan and 126 patients lived in West Japan. Consanguinity was present in 1.6% of patients (Table 1). At the time of diagnosis, the mean age was 33.4 ± 19.0 years, and the mean time between disease onset and disease diagnosis was 9.0 ± 9.8 years. Demographic data showed that 242 patients (77.8%) had no family history suggestive of FMF. The main clinical findings were present at the following frequencies: abdominal pain (171, 55.0%), arthritis (132, 42.4%), thoracic pain (119, 38.3%), myalgia (46, 14.8%), erysipelas-like erythema (32, 10.3%), and AA amyloidosis (7, 2.3%). The association with autoimmune diseases was observed in 30 (9.6%) patients

TABLE 1. Demographic and Clinical Features of 311 Patients With FMF

Feature	No. (%) (n=311)
Male/female	128/180
Consanguinity	5 (1.6%)
Age at onset (yr)*	24.2 ± 18.1
Age at diagnosis of FMF (yr)*	33.4 ± 19.0
Typical/atypical	178 / 133
Frequency of febrile attack (per mo)*0	0.9 ± 0.9
Duration of fever attack (d)*	3.4 ± 2.6
Thoracic pain	119 (38.3%)
Abdominal pain	171 (55.0%)
Arthritis	132 (42.4%)
Erysipelas-like erythema	32 (10.3%)
Myalgia	46 (14.8%)
AA amyloidosis	7 (2.3%)
Family history of FMF	69 (22.3%)
Autoimmune disease	30 (9.6%)
MEFV mutations	286 (92.0%)
Exon10 mutations	126 (40.5%)
Homozygotes (exon10)	10 (3.2%)
Compound heterozygotes	179 (57.6%)
Heterozygotes	97 (31.2%)
No. of patients prescribed colchicine	271 (87.1%)
Effective	249 (91.9%)
Ineffective	8 (3.0%)
Discontinued due to adverse effects	5 (1.8%)
Unknown	9 (3.3%)
Mean dose*	0.89 ± 0.55 mg/d

*Mean ± SD.

(rheumatoid arthritis 8; Adult-onset Still disease 4; Behçet disease 4; dermatomyositis 3; systemic lupus erythematosus 2; Basedow disease 1; idiopathic thrombocytopenic purpura 1; Kawasaki disease 1; Kikuchi disease 1; multiple sclerosis 1; polymyalgia rheumatica 1; Sjögren syndrome 2; ulcerative colitis 1). Colchicine was administered orally to 271 patients (87.1%), and a favorable therapeutic effect was seen in 249 patients (91.1%). Forty patients (12.9%) had not yet been treated with colchicine or information was not obtained in the survey. The mean dose of colchicine was 0.89 ± 0.55 mg/d. Our study population contained 59 pediatric patients (aged ≤16 yr) with FMF. The frequencies of the set of criteria for the diagnosis of FMF in childhood[34] were

as follows; fever (57/59, 96.6%), abdominal pain (38/59, 64.4%), chest pain (19/59, 32.2%), arthritis (19/59, 32.2%), and family history of FMF (13/59, 22.0%).

Mutational Analysis

Of the total 311 FMF patients, 178 displayed a typical FMF phenotype, and 133 an atypical FMF phenotype according to the Tel Hashomer criteria.[13] The distribution of the MEFV genotypes in patients with typical and atypical FMF is presented in Table 2. The detected mutations were heterogeneous and included M694I, E148Q, L110P, P369S, R408Q, and E84K. The allele frequencies

TABLE 2. MEFV Genotypes in FMF Patients With Typical or Atypical Phenotype

| MEFV Genotype	No. (%) (n=311)	Typical (n=178)	Atypical (n=133)
M694I/M694I	10 (3.2%)	10	
M694I/normal	29 (9.3%)	28	1
M694I/L110P	2 (0.6%)	2	
M694I/E148Q	50 (16.1%)	42	8
M694I/S503C	1 (0.3%)	1	
M694I/P715L	1 (0.3%)	1	
M694I/I740V	1 (0.3%)	1	
M694I/W750R	1 (0.3%)		1
M694I/E148Q/L110P	28 (9.0%)	23	5
M694I/E148Q/E148Q	1 (0.3%)	1	
M694I/E148Q/E148Q/L110P/L110P	1 (0.3%)	1	
M680I/E148Q/L110P	1 (0.3%)	1	
S503C/normal	2 (0.6%)	1	1
R354Q/normal	1 (0.3%)		1
P369S/R408Q	14 (4.5%)	1	13
E148Q/L110P/P369S	1 (0.3%)		1
E148Q/P369S/R408Q	12 (3.9%)	4	8
E225K/P369S/R408Q	1 (0.3%)	1	
G304R/P369S/R408Q	1 (0.3%)		1
E148Q/L110P/P369S/R408Q	1 (0.3%)		1
E148Q/E148Q/P369S/R408Q	6 (1.9%)	2	4
E148Q/R202Q/P369S/R408Q	1 (0.3%)		1
E148Q/G304R/P369S/R408Q	1 (0.3%)	1	
E148Q/normal	45 (14.5%)	21	24
R202Q/normal	6 (1.9%)	1	5
G304R/normal	4 (1.3%)	1	3
E148Q/E148Q	4 (1.3%)	3	1
G304R/G304R	1 (0.3%)		1
E148Q/L110P	26 (8.4%)	10	16
E148Q/R202Q	2 (0.6%)	1	1
E148Q/G304R	1 (0.3%)		1
E148Q/S503C	2 (0.6%)		2
E148Q/E148Q/L110P	6 (1.9%)	1	5
E148Q/L110P/L110P	1 (0.3%)	1	
E148Q/L110P/R202Q	2 (0.6%)		2
E148Q/L110P/G304R	1 (0.3%)		1
E148Q/E148Q/L110P/L110P	3 (1.0%)		3
E84K/normal	10 (3.2%)	4	6
E84K/E148Q	1 (0.3%)	1	
E84K/R410H	2 (0.6%)	2	
E84K/E148Q/L110P	2 (0.6%)	1	1
Normal	25 (8.0%)	10	15
Total (%)	**311**	**178 (57.2%)**	**133 (42.8%)**

— 106 —
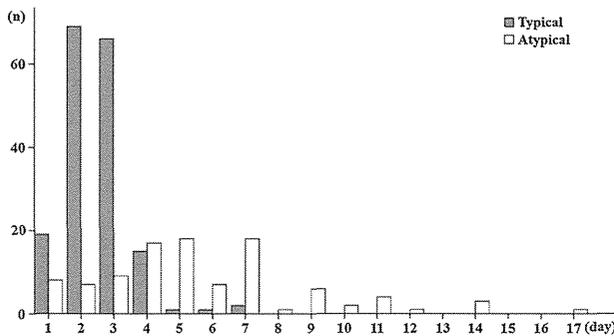
FIGURE 1. Distribution of febrile attack periods in patients with typical or atypical FMF phenotypes.

of M694I, R408Q, P369S, G304R, R202Q, E148Q, and E84K were 21.7%, 5.9%, 6.1%. 1.6%, 1.8%. 35.4%, and 2.4%, respectively, in FMF patients, compared to those in healthy Japanese subjects of 0%, 3.3%, 4.0%. 2.7%, 3.3%. 23.3%, and 1.3%, respectively, as described previously.[15] The allele frequencies were similar between the 2 groups except the M694I mutation.

Clinical Features of Different FMF Phenotypes (Typical vs. Atypical)

The distribution of febrile attack durations is shown in Figure 1. Patients with atypical FMF had variable durations, compared to the limited durations of patients with typical FMF.

We compared the demographic and genetic data between patients with the different phenotypes (typical vs. atypical). Variables that were significantly different between the 2 groups in the univariate analysis are shown in Table 3. These factors were assessed by multivariate analysis to determine whether they independently affected the typical FMF phenotype. Our best fit model was obtained through logistic regression; we found that the presence of durations of febrile attacks ≤ 3 d ($p < 0.0001$; odds ratio [OR], 44.8; 95% confidence interval [CI], 17.7–113.5) and MEFV exon 10 mutations ($p < 0.0001$; OR, 10.4; 95% CI, 3.3–32.8) predicted the typical FMF phenotype (Table 4).

Genotype/Phenotype Correlations

We analyzed the correlation between the phenotype (typical vs. atypical) and MEFV genotype using registered FMF patients. Japanese patients had a higher prevalence of the high-penetrance mutation M694I, and low-penetrance mutations in MEFV exons 1, 2, and 3 (E84K, L110P, E148Q, R202Q, G304R, P369S, R408Q). Based on these considerations, we further investigated the patient's phenotype according to the presence of higher and/or lower penetrance of MEFV mutations. Most patients carrying 1 or 2 high-penetrance mutations had the typical FMF phenotype, while, by contrast, the typical FMF phenotype percentage was slightly decreased in patients carrying combined high- and low-penetrance mutations. In contrast to the patients carrying high-penetrance mutations, more than half of the patients carrying 1 or 2 low-penetrance mutations and no detectable mutation presented with the atypical FMF phenotype (Figure 2).

Influence of the Number of MEFV Mutations on Clinical Phenotype

Although FMF is classically considered to be an autosomal recessive disease, the presence of a single mutation is often associated with a classic FMF phenotype, including the response to colchicine. We therefore analyzed the difference in clinical presentation between patients carrying 2 MEFV mutations and those with a single or no mutation. One hundred eighty-nine (60.8%) of 311 patients carried 2 or more than 2 MEFV mutations, 122 (39.2%) carried 1 or no detectable MEFV mutation. Most clinical manifestations did not differ between these 2 groups, except for the age of disease onset, the frequencies of febrile attack, and the presence of thoracic pain (Table 5).

DISCUSSION

Since the identification of MEFV as the gene mutated in FMF,[1,7] genetic analysis has become useful for confirming the diagnosis made traditionally by clinical findings.[2,13] Analysis of FMF patients in various countries has revealed patients with homozygous and compound heterozygous mutations, others with single mutations, and some with none of the studied mutations.[17,30] Indeed, we encountered Japanese FMF patients with only a single

TABLE 3. Comparison of Clinical Features in Patients With Typical or Atypical FMF Phenotype (Univariate Analysis)

Feature	Typical No. (%) (n=178)	Atypical No. (%) (n=133)	P
Male/female	81/96	47/84	0.082
Consanguinity	3 (1.7%)	2 (1.5%)	0.635
Age at onset (yr)*	21.9 ± 16.3	27.3 ± 20.0	0.019
Frequency of febrile attack (per mo)*	1.1 ± 0.9	0.8 ± 0.8	P < 0.0001
Duration of febrile attack (d)*	2.3 ± 1.0	5.4 ± 3.2	P < 0.0001
Thoracic pain	88 (49.4%)	31 (23.3%)	P < 0.0001
Abdominal pain	117 (65.7%)	54 (40.6)	P < 0.0001
Arthritis	64 (36.0%)	68 (51.1%)	0.007
Erysipelas-like erythema	11 (6.2%)	21 (15.8%)	0.006
Myalgia	20 (11.2%)	26 (19.5%)	0.041
Family history of FMF	50 (28.1%)	19 (14.3%)	0.004
Autoimmune diseases	14 (7.9%)	16 (12.0%)	0.218
Exon 10 mutations (+)	111 (62.4%)	15 (11.3%)	P < 0.0001
Exon 3 mutations (+)	11 (6.2%)	30 (22.6%)	P < 0.0001

*Mean ± SD.

TABLE 4. Comparison of Selected Variables for Typical FMF Phenotype (Multivariate Analysis)

Variable	P	OR (95% CI)
Age at onset (≤20 yr)	0.404	0.668 (0.259–1.725)
Frequency of febrile attack (≥1/mo)	0.360	1.473 (0.643–3.375)
Duration of febrile attack (≤3 d)	P < 0.0001	44.779 (17.670–113.479)
Thoracic pain	0.833	0.902 (0.347–2.346)
Abdominal pain	0.040	2.548 (1.046–6.210)
Arthritis	0.136	2.021 (0.801–5.102)
Erysipelas-like erythema	0.719	0.759 (0.168–3.418)
Myalgia	0.237	0.510 (0.167–1.558)
Family history of FMF	0.830	0.884 (0.288–2.717)
Exon 10 mutations (+)	P < 0.0001	10.445 (3.330–32.763)
Exon 3 mutations (+)	0.803	0.855 (0.250–2.921)

mutation or low-penetrance MEFV exon 2 or 3 mutations.[16] This is especially common among populations with a high frequency of low-penetrance mutation carriers.[30]

In the current study, 43% of Japanese patients with FMF were classified as having atypical FMF according to the Tel Hashomer diagnostic criteria.[13] These patients exhibited unique clinical manifestations, including some that are atypical FMF symptoms such as prolonged periods of febrile attacks and lower frequencies of serositis. Our data confirmed the correlation between the MEFV exon 10 mutations and the typical FMF phenotype, as well as that between MEFV exon 3 mutations and the atypical FMF phenotype in Japanese patients. Based on genetic analysis, the prevalence of the typical FMF phenotype was correlated with MEFV genotype, increasing from patients who carried no MEFV mutations or low-penetrance MEFV mutations to those who carried high-penetrance MEFV mutations. Multivariate analysis revealed that MEFV exon 10 mutations were significantly associated with the typical FMF phenotype in Japanese patients. This contrasts with a previous study in which only the M694V variant was associated with FMF disease severity.[23]

The main limitation of the current study is the lack of evaluation of disease severity; however, the MEFV genotype could be linked to the FMF clinical phenotype of Japanese patients as demonstrated in Middle Eastern countries.[21] Although the dose effects of MEFV mutations to disease phenotype were minimal, the presence of a high-penetrance MEFV mutation (M694I) extensively affected the FMF phenotype. Our findings suggest that MEFV genotypes are useful to distinguish atypical from typical FMF patients. However, genetic testing has a limited diagnostic value, and the diagnosis of FMF remains clinical despite the understanding of the genotype-phenotype correlation. Nevertheless, our data shed light on the contribution of MEFV genotypes to the "FMF phenotype" in Japanese patients with FMF.

On the basis of the recessive mode of inheritance, FMF patients should inherit 2 mutations in the MEFV gene. However, several investigators have assumed that some heterozygous mutation carriers have clinically symptomatic FMF.[4,5,18] Indeed, new studies have cast considerable doubt on whether FMF is a traditional autosomal recessive disease.[26] Several possibilities including the presence of mutations in another autoinflammatory gene, epigenetic or post-translational modifications, and environmental factors have been suggested.[5,17,32] Additionally, patients carrying MEFV mutations with low penetrance do not present with classical FMF and suffer from mild or atypical FMF characterized by episodic arthritis without fever, or febrile attacks without serositis.[3,20,25] We suggest that appropriate molecular tests for MEFV could be

useful for classifying the FMF phenotype in Japanese patients. Recent data from a pyrin knock-in mouse suggest that FMF is the result of gain-of-function mutations in pyrin that lead to interleukin-1β activation.[11] This may account for FMF patients with only 1 identifiable MEFV mutation who present with FMF disease that is responsive to colchicine. This has been observed in patients with low-penetrance mutations in MEFV exons 1–3.

There has been some debate about the use of clinical versus genetic criteria, as the diagnosis of FMF cannot be made on the basis of genetic testing alone.[6] Some patients with FMF diagnosed by clinical findings have only 1 demonstrable mutation, and a small number of patients have no identifiable mutations. In addition, the Tel Hashomer clinical criteria do not clearly distinguish typical from atypical FMF.[10] Our results suggest that combined clinical investigations and molecular analysis are useful to discriminate the different phenotypes of FMF.

In summary, we confirmed that MEFV exon 10 mutations are associated with the more typical FMF phenotype. Conversely, more than half of the Japanese FMF patients without MEFV exon 10 mutations presented with an atypical FMF phenotype. Further studies involving a multicentric FMF registration are needed to establish a correlation between the MEFV genotype and various clinical phenotypes in different ethnic groups, which should be further explored in larger studies.
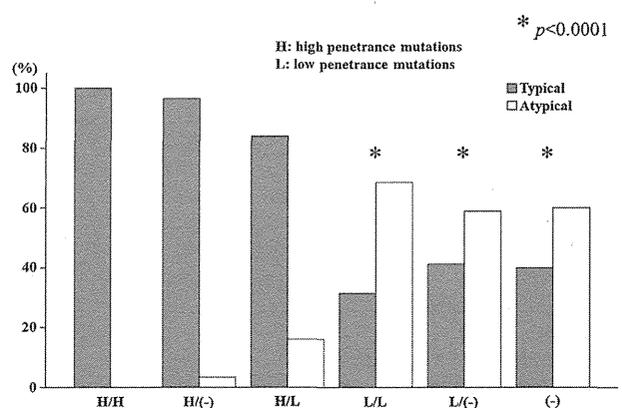

FIGURE 2. Prevalence of typical or atypical FMF phenotype in patients with high- (H) or low- (L) penetrance MEFV mutations. P values were assessed by Fisher exact test in comparison with patients having 2 high-penetrance (H/H) MEFV mutations.

TABLE 5. Clinical Features of Patients With Different Numbers of MEFV Mutations

	No. (%) of MEFV Mutations		
Feature	≥2 Mutations (n=189)	1 or No Mutation (n=122)	P
Male/female	71/117	57/63	0.091
Consanguinity	2 (1.1%)	3 (2.5%)	0.303
Age at onset (yr)*	22.0 ± 16.9	27.7 ± 19.5	0.013
Frequency of febrile attack (per mo)*	1.0 ± 0.9	0.8 ± 0.8	0.025
Duration of febrile attack (d)*	3.4 ± 2.5	3.5 ± 2.8	0.596
Thoracic pain	85 (45.0%)	34 (27.9%)	0.002
Abdominal pain	108 (57.1%)	63 (51.6%)	0.341
Arthritis	77 (40.7%)	55 (45.1%)	0.449
Erysipelas-like erythema	17 (9.0%)	15 (12.3%)	0.350
Myalgia	26 (13.8%)	20 (16.4%)	0.522
Family history of FMF	46 (24.3%)	23 (18.9%)	0.256
Autoimmune diseases	19 (11.3%)	11 (9.8%)	0.693

*Mean ± SD.

REFERENCES

1. Ancient missense mutations in a new member of the RoRet gene family are likely to cause familial Mediterranean fever. The International FMF Consortium. *Cell.* 1997;90:797–807.

2. Ben-Chetrit E, Levy M. Familial Mediterranean fever. *Lancet.* 1998;351:659–664.

3. Ben-Chetrit E, Peleg H, Aamar S, Heyman SN. The spectrum of MEFV clinical presentations—is it familial Mediterranean fever only? *Rheumatology (Oxford).* 2009;48:1455–1459.

4. Booth DR, Gillmore JD, Lachmann HJ, Booth SE, Bybee A, Soyturk M, Akar S, Pepys MB, Tunca M, Hawkins PN. The genetic basis of autosomal dominant familial Mediterranean fever. *QJM.* 2000;93:217–221.

5. Booty MG, Chae JJ, Masters SL, Remmers EF, Barham B, Le JM, Barron KS, Holland SM, Kastner DL, Aksentijevich I. Familial Mediterranean fever with a single MEFV mutation: where is the second hit? *Arthritis Rheum.* 2009;60:1851–1861.

6. Federici L, Rittore-Domingo C, Kone-Paut I, Jorgensen C, Rodiere M, Le Quellec A, Touitou I. A decision tree for genetic diagnosis of hereditary periodic fever in unselected patients. *Ann Rheum Dis.* 2006;65:1427–1432.

7. French FMF Consortium. A candidate gene for familial Mediterranean fever. *Nat Genet.* 1997;17:25–31.

8. Gershoni-Baruch R, Brik R, Shinawi M, Livneh A. The differential contribution of MEFV mutant alleles to the clinical profile of familial Mediterranean fever. *Eur J Hum Genet.* 2002;10:145–149.

9. Gershoni-Baruch R, Shinawi M, Leah K, Badarnah K, Brik R. Familial Mediterranean fever: prevalence, penetrance and genetic drift. *Eur J Hum Genet.* 2001;9:634–637.

10. Grateau G, Pecheux C, Cazeneuve C, Cattan D, Dervichian M, Goossens M, Delpech M, Amselem S, Dode C. Clinical versus genetic diagnosis of familial Mediterranean fever. *QJM.* 2000;93:223–229.

11. Chae JJ, Cho YH, Lee GS, Cheng J, Liu PP, Feigenbaum L, Katz SI, Kastner DL. Gain-of-function pyrin mutations induce NLRP3 protein-independent interleukin-1β activation and severe autoinflammation in mice. *Immunity.* 2011;34:755–768.

12. Kone-Paut I, Hentgen V, Guillaume-Czitrom S, Compeyrot-Lacassagne S, Tran TA, Touitou I. The clinical spectrum of 94 patients carrying a single mutated MEFV allele. *Rheumatology (Oxford).* 2009;48:840–842.

13. Livneh A, Langevitz P, Zemer D, Zaks N, Kees S, Lidar T, Migdal A, Padeh S, Pras M. Criteria for the diagnosis of familial Mediterranean fever. *Arthritis Rheum.* 1997;40:1879–1885.

14. Marek-Yagel D, Berkun Y, Padeh S, Abu A, Reznik-Wolf H, Livneh A, Pras M, Pras E. Clinical disease among patients heterozygous for familial Mediterranean fever. *Arthritis Rheum.* 2009;60:1862–1866.

15. Migita K, Ida H, Moriuchi H, Agematsu K. Clinical relevance of MEFV gene mutations in Japanese patients with unexplained fever. *J Rheumatol.* 2012;39:875–877.

16. Migita K, Uehara R, Nakamura Y, Yasunami M, Tsuchiya-Suzuki A, Yazaki M, Nakamura A, Masumoto J, Yachie A, Furukawa H, Ishibashi H, Ida H, Yamazaki K, Kawakami A, Agematsu K. Familial Mediterranean fever in Japan. *Medicine (Baltimore).* 2012;91:337–343.

17. Moradian MM, Sarkisian T, Ajrapetyan H, Avanesian N. Genotype-phenotype studies in a large cohort of Armenian patients with familial Mediterranean fever suggest clinical disease with heterozygous MEFV mutations. *J Hum Genet.* 2010;55:389–393.

18. Ozen S. Changing concepts in familial Mediterranean fever: is it possible to have an autosomal-recessive disease with only one mutation? *Arthritis Rheum.* 2009;60:1575–1577.

19. Padeh S, Shinar Y, Pras E, Zemer D, Langevitz P, Pras M, Livneh A. Clinical and diagnostic value of genetic testing in 216 Israeli children with Familial Mediterranean fever. *J Rheumatol.* 2003;30:185–190.

20. Ryan JG, Masters SL, Booty MG, Habal N, Alexander JD, Barham BK, Remmers EF, Barron KS, Kastner DL, Aksentijevich I. Clinical features and functional significance of the P369S/R408Q variant in pyrin, the familial Mediterranean fever protein. *Ann Rheum Dis.* 2010;69:1383–1388.

21. Samuels J, Aksentijevich I, Torosyan Y, Centola M, Deng Z, Sood R, Kastner DL. Familial Mediterranean fever at the millennium. Clinical spectrum, ancient mutations, and a survey of 100 American referrals to the National Institutes of Health. *Medicine (Baltimore).* 1998;77:268–297.

22. Savic S, Dickie LJ, Battellino M, McDermott MF. Familial Mediterranean fever and related periodic fever syndromes/autoinflammatory diseases. *Curr Opin Rheumatol.* 2012;24:103–112.

23. Shinar Y, Livneh A, Langevitz P, Zaks N, Aksentijevich I, Koziol DE, Kastner DL, Pras M, Pras E. Genotype-phenotype assessment of common genotypes among patients with familial Mediterranean fever. *J Rheumatol.* 2000;27:1703–1707.

24. Sohar E, Gafni J, Pras M, Heller H. Familial Mediterranean fever. A survey of 470 cases and review of the literature. *Am J Med.* 1967;43:227–253.

25. Soriano A, Manna R. Familial Mediterranean fever: new phenotypes. *Autoimmun Rev.* 2012;12:31–37.

26. Stoffels M, Szperl A, Simon A, Netea MG, Plantinga TS, van Deuren M, Kamphuis S, Lachmann HJ, Cuppen E, Kloosterman WP, Frenkel J, van Diemen CC, Wijmenga C, van Gijn M, van der Meer JW. MEFV mutations affecting pyrin amino acid 577 cause autosomal dominant autoinflammatory disease. *Ann Rheum Dis.* 2014;73:455–461. Epub 2013 Mar 16.

27. Tanaka M, Migita K, Miyashita T, Maeda Y, Nakamura M, Komori A, Ishibashi H, Eguchi K, Kikuchi M, Hirayama K, Yasunami M. Coexistence of familial Mediterranean fever and Sjogren's syndrome in a Japanese patient. *Clin Exp Rheumatol.* 2007;25:792.

28. Tchernitchko D, Moutereau S, Legendre M, Delahaye A, Cazeneuve C, Lacombe C, Grateau G, Amselem S. MEFV analysis is of particularly weak diagnostic value for recurrent fevers in Western European Caucasian patients. *Arthritis Rheum.* 2005;52:3603–3605.

29. Tomiyama N, Higashiuesato Y, Oda T, Baba E, Harada M, Azuma M, Yamashita T, Uehara K, Miyazato A, Hatta K, Ohya Y, Iseki K, Jinno Y, Takishita S. MEFV mutation analysis of familial Mediterranean fever in Japan. *Clin Exp Rheumatol.* 2008;26:13–17.

30. Touitou I. The spectrum of familial Mediterranean fever (FMF) mutations. *Eur J Hum Genet.* 2001;9:473–483.

31. Touitou I, Lesage S, McDermott M, Cuisset L, Hoffman H, Dode C, Shoham N, Aganna E, Hugot JP, Wise C, Waterham H, Pugnere D, Demaille J, Sarrauste de Menthiere C. Infevers: an evolving mutation database for auto-inflammatory syndromes. *Hum Mutat.* 2004;24:194–198.

32. Touitou I, Picot MC, Domingo C, Notarnicola C, Cattan D, Demaille J, Kone-Paut I. The MICA region determines the first modifier locus in familial Mediterranean fever. *Arthritis Rheum.* 2001;44:163–169.

33. Tsuchiya-Suzuki A, Yazaki M, Nakamura A, Yamazaki K, Agematsu K, Matsuda M, Ikeda S. Clinical and genetic features of familial Mediterranean fever in Japan. *J Rheumatol.* 2009;36:1671–1676.

34. Yalcinkaya F, Ozen S, Ozcakar ZB, Aktay N, Cakar N, Duzova A, Kasapcopur O, Elhan AH, Doganay B, Ekim M, Kara N, Uncu N, Bakkaloglu A. A new set of criteria for the diagnosis of familial Mediterranean fever in childhood. *Rheumatology (Oxford).* 2009;48:395–398.

Enhanced Chondrogenesis of Induced Pluripotent Stem Cells From Patients With Neonatal-Onset Multisystem Inflammatory Disease Occurs via the Caspase 1–Independent cAMP/Protein Kinase A/CREB Pathway

Koji Yokoyama,[1] Makoto Ikeya,[1] Katsutsugu Umeda,[1] Hirotsugu Oda,[2] Seishiro Nodomi,[1] Akira Nasu,[1] Yoshihisa Matsumoto,[3] Kazushi Izawa,[1] Kazuhiko Horigome,[4] Toshimasa Kusaka,[1] Takayuki Tanaka,[1] Megumu K. Saito,[1] Takahiro Yasumi,[1] Ryuta Nishikomori,[1] Osamu Ohara,[5] Naoki Nakayama,[6] Tatsutoshi Nakahata,[1] Toshio Heike,[1] and Junya Toguchida[1]

Objective. Neonatal-onset multisystem inflammatory disease (NOMID) is a dominantly inherited autoinflammatory disease caused by NLRP3 mutations. NOMID pathophysiology is explained by the NLRP3 inflammasome, which produces interleukin-1β (IL-1β). However, epiphyseal overgrowth in NOMID is resistant to anti–IL-1 therapy and may therefore occur independently of the NLRP3 inflammasome. This study was undertaken to investigate the effect of mutated NLRP3 on chondrocytes using induced pluripotent stem cells (iPSCs) from patients with NOMID.

Methods. We established isogenic iPSCs with wild-type or mutant NLRP3 from 2 NOMID patients with NLRP3 somatic mosaicism. The iPSCs were differentiated into chondrocytes in vitro and in vivo. The phenotypes of chondrocytes with wild-type and mutant NLRP3 were compared, particularly the size of the chondrocyte tissue produced.

Results. Mutant iPSCs produced larger chondrocyte masses than wild-type iPSCs owing to glycosaminoglycan overproduction, which correlated with increased expression of the chondrocyte master regulator SOX9. In addition, in vivo transplantation of mutant cartilaginous pellets into immunodeficient mice caused disorganized endochondral ossification. Enhanced chondrogenesis was independent of caspase 1 and IL-1, and thus the NLRP3 inflammasome. Investigation of the human *SOX9* promoter in chondroprogenitor cells revealed that the CREB/ATF-binding site was critical for SOX9 overexpression caused by mutated NLRP3. This was supported by increased levels of cAMP and phosphorylated CREB in mutant chondroprogenitor cells.

Conclusion. Our findings indicate that the intrinsic hyperplastic capacity of NOMID chondrocytes is dependent on the cAMP/PKA/CREB pathway, independent of the NLRP3 inflammasome.

302

Systemic autoinflammatory syndromes are caused by defects in the innate immune system, especially pattern-recognition receptors, which result in uncontrolled inflammatory responses (1). Neonatal-onset multisystem inflammatory disease (NOMID) is a systemic autoinflammatory disease caused by NLRP3 mutation (2). The clinical features of NOMID include neonatal-onset persistent inflammation, urticarial rash, chronic aseptic meningitis, and arthropathy characterized by tumor-like expansive lesions in epiphyseal portions of long bones (3). NLRP3 is mainly expressed in hematopoietic cells, especially monocyte/macrophages, and in chondrocytes (4). In monocyte/macrophages, once NLRP3 is activated by its ligand, a multiprotein complex called the NLRP3 inflammasome forms, resulting in the activation of caspase 1, which cleaves pro–interleukin-1β (IL-1β) into active IL-1β (5–8).

The molecular mechanism by which NOMID-associated NLRP3 mutations lead to the activation of the NLRP3 inflammasome has not been fully elucidated. However, it is hypothesized that mutated NLRP3 can trigger the formation of the NLRP3 inflammasome independently of ligand binding, which causes dysregulated IL-1β secretion and uncontrolled multisystem inflammation. This hypothesis is supported by the fact that a targeted therapy against IL-1β effectively controls systemic inflammation in NOMID (9–11). However, epiphyseal overgrowth in NOMID is resistant to anti–IL-1 therapy (12).

Sequential radiologic imaging and histologic analyses of tissue biopsy specimens suggest that the main pathophysiology of NOMID arthropathy is not inflammation but disorganization of cartilage cell columns that leads to tumor-like expansive lesions (13). These clinical and pathologic findings suggest that mutant NLRP3 induces epiphyseal overgrowth in NOMID via mechanisms unrelated to the NLRP3 inflammasome. However, the function of NLRP3 in chondrocytes has not been elucidated, let alone the mechanism underlying epiphyseal overgrowth in NOMID.

Cartilage is a flexible connective tissue in the skeletal system and consists of chondrocytes and extracellular matrix (ECM). The growth plate consists of a column of chondrocytes that separate the epiphysis and metaphysis of a long bone. The primary function of these chondrocytes is to provide a cartilage template on which bone can form through endochondral ossification. In the growth plate, maturing chondrocytes are organized into resting, proliferating, prehypertrophic, and hypertrophic zones. Growth factor signaling stimulates mesenchymal progenitor cells in the resting zone to

proliferate, upon which they move to the proliferating zone. These cells subsequently produce cartilage-specific ECM consisting of type II collagen and type XI collagens, and proteoglycans, such as aggrecan and cartilage oligomeric matrix protein. These cells then exit the cell cycle, differentiate, become hypertrophic, produce type X collagen and matrix metalloproteinases, and finally undergo apoptosis. The remaining cartilaginous matrix is mineralized and provides a scaffold on which bone can form (14,15).

It is difficult to obtain bone tissues from NOMID patients due to ethical reasons. Moreover, osteochondrogenic progenitor cells often cannot be obtained from postnatal human tissues in sufficient quantities, while acquiring such cells in sufficient quantities from human fetuses or embryos is ethically challenging. Furthermore, although a mass-like lesion called a "spike" is observed in mouse models of NOMID arthropathy (16), these models do not recapitulate the epiphyseal overgrowth observed in NOMID. These issues have prevented elucidation of the pathophysiologic mechanism underlying epiphyseal overgrowth in NOMID. In this study, we applied a newly developed chondrocyte differentiation system to induced pluripotent stem cells (iPSCs) derived from NOMID patients. This system allowed chondrocytes to be obtained in sufficient quantities to directly study the effect of mutated NLRP3 on chondrocyte phenotypes, focusing on the involvement of the NLRP3 inflammasome and the master regulator of chondrocyte differentiation, SOX9.

MATERIALS AND METHODS

Cell culture. Undifferentiated iPSCs from 2 NOMID patients with NLRP3 somatic mosaicism (p.Tyr570Cys and p.Gly307Ser) were established as previously described (17). From each patient, at least 3 clones of iPSCs with mutant or wild-type NLRP3 were established. In all experiments, mutant and wild-type isogenic cells were compared (3). Details of the procedure for culture of undifferentiated iPSCs and chondrogenic differentiation are available from the author upon request. The iPSCs were seeded onto a Matrigel (Becton Dickinson)–coated dish, cultured in mTeSR medium (Stem-Cell Technologies) for 9 days, and then transferred to initial differentiation medium. This medium was changed once on day 3. On day 6, a single-cell suspension was prepared with 0.05% trypsin-EDTA. These cells were plated onto fibronectin-coated dishes, cultured in chondroprogenitor medium, and passaged every 3 days. We called these cells chondroprogenitor cells. For chondrogenesis, chondroprogenitor cells that had been passaged 3–5 times were used (Figure 1A).

Chondrogenesis assay. Serum-free chondrogenic medium has been described previously (18). Two-dimensional
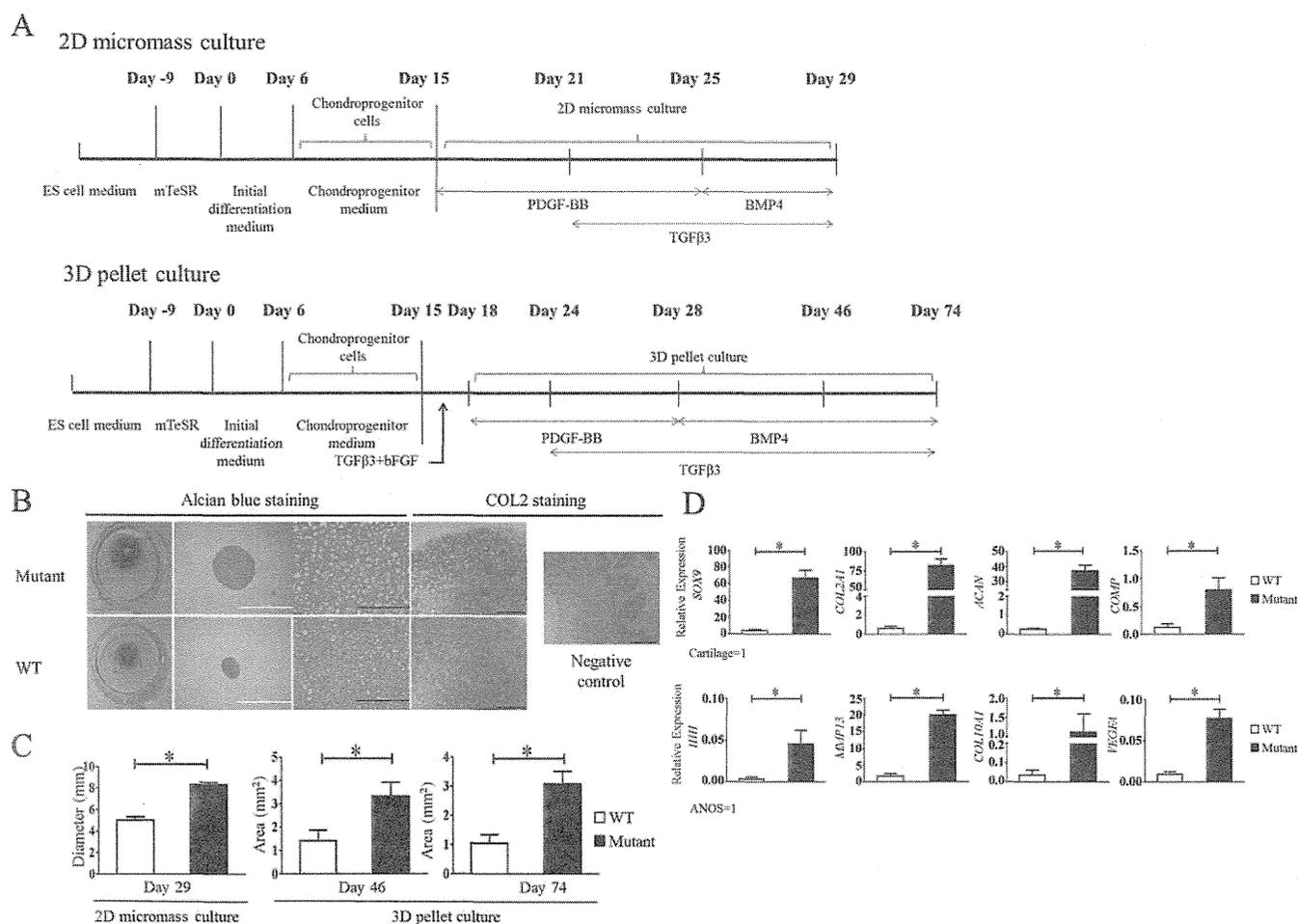
Figure 1. Successful differentiation of chondrocytes from induced pluripotent stem cells (iPSCs) with wild-type (WT) or mutant NLRP3 obtained from a patient with neonatal-onset multisystem inflammatory disease. **A,** Schematic representation of the culture conditions used to differentiate chondrocytes from iPSCs. **B,** Immunohistochemical staining of chondrocytes differentiated from iPSCs. Alcian blue staining of the 2-dimensional (2-D) micromass culture, Alcian blue staining of the 3-dimensional (3-D) pellet culture, higher-magnification images of Alcian blue staining of the 3-D pellet culture, anti–type II collagen (anti-COL2) antibody staining of the 3-D pellet culture, and anti–type II collagen antibody staining of mouse bladder (negative control) are shown. White bars = 2.0 mm; black bars = 0.2 mm. **C,** Quantitative analysis of the sizes of chondrocyte tissue masses in 2-D micromass cultures and 3-D pellet cultures. **D,** Cartilage-specific gene expression in 3-D pellet cultures. Expression of mRNA for each gene is shown relative to that in human cartilage (for *SOX9*, *COL2A1*, *ACAN*, and *COMP*) or the osteosarcoma cell line ANOS (for *IHH*, *MMP13*, *COL10A1*, and *VEGFA*), which were both set at 1. Bars in C and D show the mean ± SEM of 3 independent clones, from which duplicate measurements (C) or triplicate measurements (D) were obtained. Data are representative of 3 independent experiments and were obtained using iPSCs from patient 1 (p.Tyr570Cys); similar data were obtained using iPSCs from patient 2 (p.Gly307Ser). ∗ = $P < 0.05$. ES = embryonic stem; PDGF-BB = platelet-derived growth factor BB; BMP-4 = bone morphogenetic protein 4; TGFβ3 = transforming growth factor β3; bFGF = basic fibroblast growth factor.

(2-D) micromass culture was performed by spotting a 5-μl droplet of chondroprogenitor cells (1.5×10^5) onto the well of a fibronectin-coated 24-well plate in serum-free chondrogenic medium supplemented with 40 ng/ml of platelet-derived growth factor BB (PDGF-BB; R&D Systems) and 1% fetal calf serum. The medium was changed every 3 days. Beginning on day 21, 10 ng/ml of transforming growth factor β3 (TGFβ3; R&D Systems) was added, and beginning on day 25, 40 ng/ml

of PDGF-BB was replaced with 50 ng/ml of bone morphogenetic protein 4 (Wako). For 3-dimensional (3-D) pellet cultures, chondroprogenitor cells were passaged once in chondroprogenitor medium containing 5 ng/ml of basic fibroblast growth factor and 10 ng/ml of TGFβ3, and then cultured for 3 days. Aliquots of 2.5×10^5 cells were centrifuged to form pellets, which were cultured in 0.5 ml of serum-free chondrogenic medium supplemented with specific factors as outlined

above. Fixation and staining of the 2-D micromass and 3-D pellet cultures were performed as previously described (18). Glycosaminoglycan (GAG) and sulfated proteoglycan levels and DNA content were quantified as previously described (19).

Chondrogenesis in vivo. Cartilaginous pellets formed by 3-D cell pellet cultures over 20 days were wrapped in a 0.5 cm × 1 cm Gelfoam (Pfizer) and transplanted beneath the dorsal skin of immunodeficient NOD/Shi-scid, IL-2Rγ(null) (NOG) mice. Four weeks later, cartilage and bone particles were harvested, fixed with paraformaldehyde for 24 hours, embedded in plastic, sectioned, and stained with hematoxylin and eosin (H&E), von Kossa, or Alcian blue, as previously reported (18).

Enzyme-linked immunosorbent assay (ELISA) and Western blotting. The concentration of cAMP was measured using an ELISA (Cell Signaling Technology). Antibodies against CREB, phosphorylated CREB (Cell Signaling), and β-actin (Santa Cruz Biotechnology) were used for Western blotting, as previously described (20).

Gene expression profiling. Total RNA was extracted and reverse-transcribed to cDNA using Superscript III reverse transcriptase (Invitrogen) according to the manufacturer's protocol. Quantitative reverse transcriptase–polymerase chain reaction was performed as previously described (19). The expression levels of each gene from duplicate or triplicate reactions were normalized against the level of the *BACT* transcript and are shown relative to their expression in the osteosarcoma cell line ANOS (21) or a human articular cartilage sample.

Reporter assay for the human SOX9 promoter. To measure the activity of the human *SOX9* promoter in chondroprogenitor cells, the 5'-untranslated region (5'-UTR) of the human *SOX9* gene (−927 to +84 bp) was inserted into a pGL3-luciferase reporter plasmid (Promega), as previously described (22). Site-directed mutagenesis of the known transcription factor–binding sites of the human *SOX9* promoter was performed as previously described (23). The residue was mutated to the nucleotide that was least likely to be at this position, based on consensus sequences in the JASPAR transcription database (24). Sequence information is provided in Supplementary Figure 1, available on the *Arthritis & Rheumatology* web site at http://onlinelibrary.wiley.com/doi/10.1002/art.38912/abstract. Chondroprogenitor cells were plated at a density of 50,000 cells/well in 6-well plates, transfected with 2 μg of DNA/well using the FuGene 6 transfection reagent, and harvested 24 hours after transfection. Luciferase activity was measured as previously described (23). Additionally, 10 μM forskolin (Sigma) and 10 μM SQ22536 (Sigma) was used to activate and inhibit adenylate cyclase, respectively.

Ethics approval. This study was approved by the ethics committee of Kyoto University and was performed in accordance with the Declaration of Helsinki. A sample of human articular cartilage was obtained from a patient who underwent knee surgery and provided informed consent that the sample could be used for research purposes.

Statistical analysis. Data were analyzed using Student's *t*-test. *P* values less than 0.05 were considered significant.

RESULTS

Production of a large cartilaginous mass by chondrocytes differentiated from iPSCs with mutated NLRP3. To investigate the pathophysiology of NOMID arthropathy, we attempted to recapitulate this phenotype by using chondrocytes that were differentiated from iPSCs derived from patients with NOMID. We obtained iPSCs from 2 NOMID patients with arthropathy who had *NLRP3* somatic mosaicism, as previously described (17). We established isogenic iPSC clones that had mutated or wild-type NLRP3, which allowed us to examine the effects of NLRP3 mutations in the same genetic background (25,26).

To produce chondrocytes from these iPSCs, we used a protocol in which chondrocytes are obtained from cells of neural crest character (details are available from the author upon request) (Figure 1A). We performed 2 chondrogenic assays, a 2-D micromass culture assay and a 3-D pellet assay. The former is suitable for experiments with exogenous inhibitors or activators, whereas the latter generates more mature chondrocytes for in vivo transplantation assay. First, we confirmed the phenotype of cartilage samples by performing Alcian blue staining, which labels ECM excreted by chondrocytes, and immunostaining for type II collagen, which is specifically expressed in chondrocytes (Figure 1B). After culture in chondrogenic medium, cells derived from wild-type and mutant iPSCs were positive for Alcian blue and type II collagen, which confirmed that the iPSCs had successfully differentiated into chondrocytes. Importantly, the 2-D micromass and 3-D pellet samples derived from mutant iPSCs were significantly larger than those derived from wild-type iPSCs, up to day 74 of culture (Figures 1B and C).

Next, we examined the expression of mRNA for cartilage-related genes expressed in proliferating chondrocytes (early markers; *SOX9, COL2A1, ACAN*, and *COMP*) and those expressed in hypertrophic chondrocytes (late markers; *IHH, MMP13, COL10A1*, and *VEGFA*) in samples obtained by the method described above (Figure 1D). These genes were expressed in 3-D pellet samples obtained from mutant and wild-type iPSCs, further indicating that chondrocyte differentiation was successful and that 3-D pellets contained chondrocytes at various differentiation stages. The expression levels of both early and late chondrogenic markers were significantly higher in mutant samples than in wild-type samples (Figure 1D). Taken together, these data show that chondrocytes were successfully differentiated in
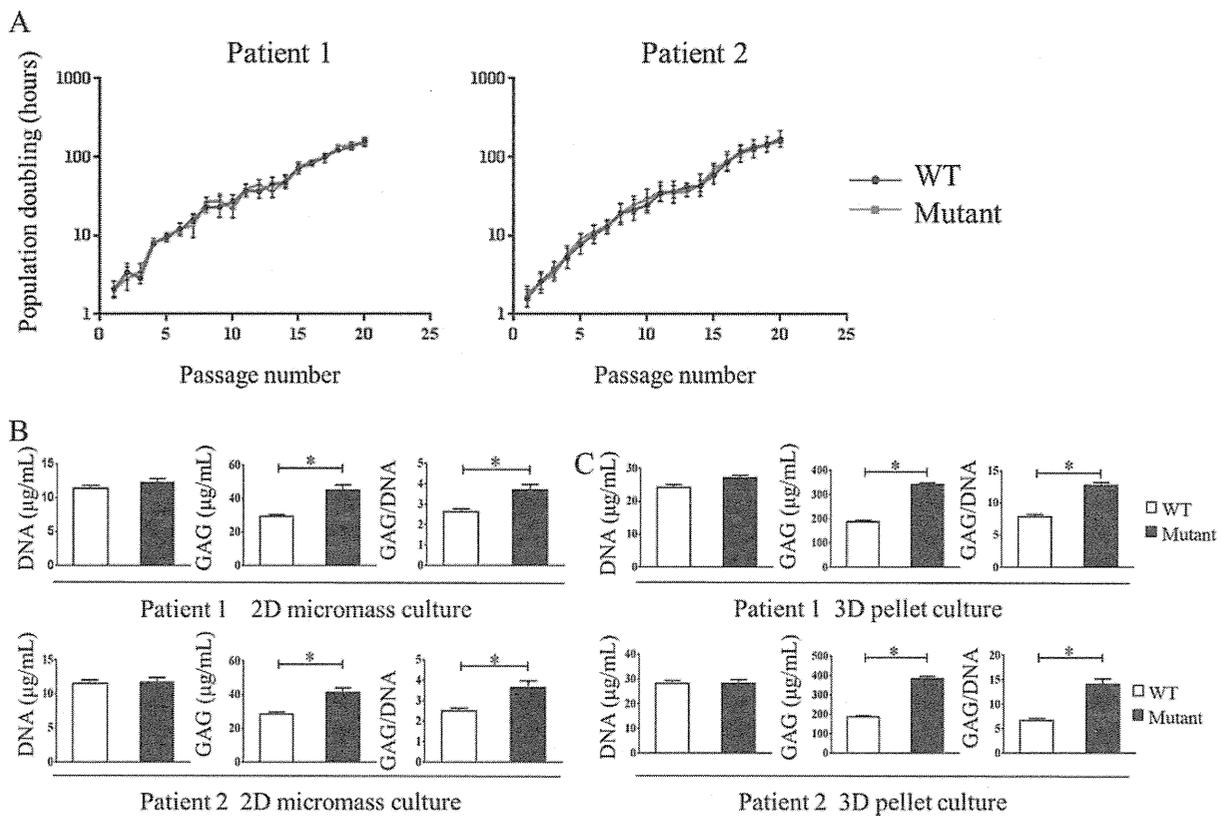
Figure 2. Formation of large cartilaginous masses by mutant iPSCs from patients with neonatal-onset multisystem inflammatory disease is due to the overproduction of extracellular matrix and not due to increased cell proliferation. **A,** Growth curves of chondroprogenitor cells differentiated from mutant and wild-type iPSCs. Values are the mean $\pm$ SEM of 3 independent clones, from which duplicate measurements were obtained. **B** and **C,** DNA concentration, glycosaminoglycan (GAG) concentration, and the ratio of GAG concentration to DNA concentration in 2-D micromass (**B**) and 3-D pellet (**C**) cultures. Bars show the mean $\pm$ SEM of 3 independent clones, from which triplicate (**B**) or duplicate (**C**) measurements were obtained. Data are representative of 3 independent experiments with consistent results. $* = P < 0.05$. See Figure 1 for other definitions.

vitro from iPSCs derived from NOMID patients, and that chondrocytes differentiated from iPSCs with mutant *NLRP3* produce large cartilaginous masses in vitro. They also demonstrate that the entire chondrocyte differentiation process, from precursors to late chondrocytes, is enhanced in mutant cells compared to wild-type cells.

The production of large cartilaginous masses by mutant iPSCs is due to ECM overproduction, not to increased cell proliferation. We next sought to determine what causes the chondrocyte masses derived from mutant iPSCs to be larger than those derived from wild-type iPSCs. First, we analyzed the proliferation potential of chondroprogenitor cells. Population doubling time did not significantly differ between mutant and wild-type chondroprogenitor cells up to 15 passages, after which the cells stopped proliferating (Figure 2A). Next, we determined the number of differentiated chondrocytes by analyzing DNA content and GAG produc-

tion, which is a major cartilaginous ECM component. In 2-D micromass and 3-D pellet cultures, the DNA content in differentiated chondrocyte tissue derived from mutant and wild-type iPSCs did not significantly differ. This suggests that a similar number of chondrocytes were produced from mutant and wild-type iPSCs. In contrast, chondrocytes derived from mutant iPSCs produced more GAG than those derived from wild-type iPSCs in 2-D micromass culture (Figure 2B) and 3-D pellet culture (Figure 2C). These data indicate that the larger amount of chondrocyte tissue produced from mutant iPSCs is not due to an increased number of chondrocytes, but to an increased amount of cartilaginous ECM produced per cell.

In vivo differentiation of chondrocytes from mutant iPSCs reveals dysregulated endochondral ossification. Radiologic examination of affected long bones in NOMID patients shows enlargement of the epiphysis
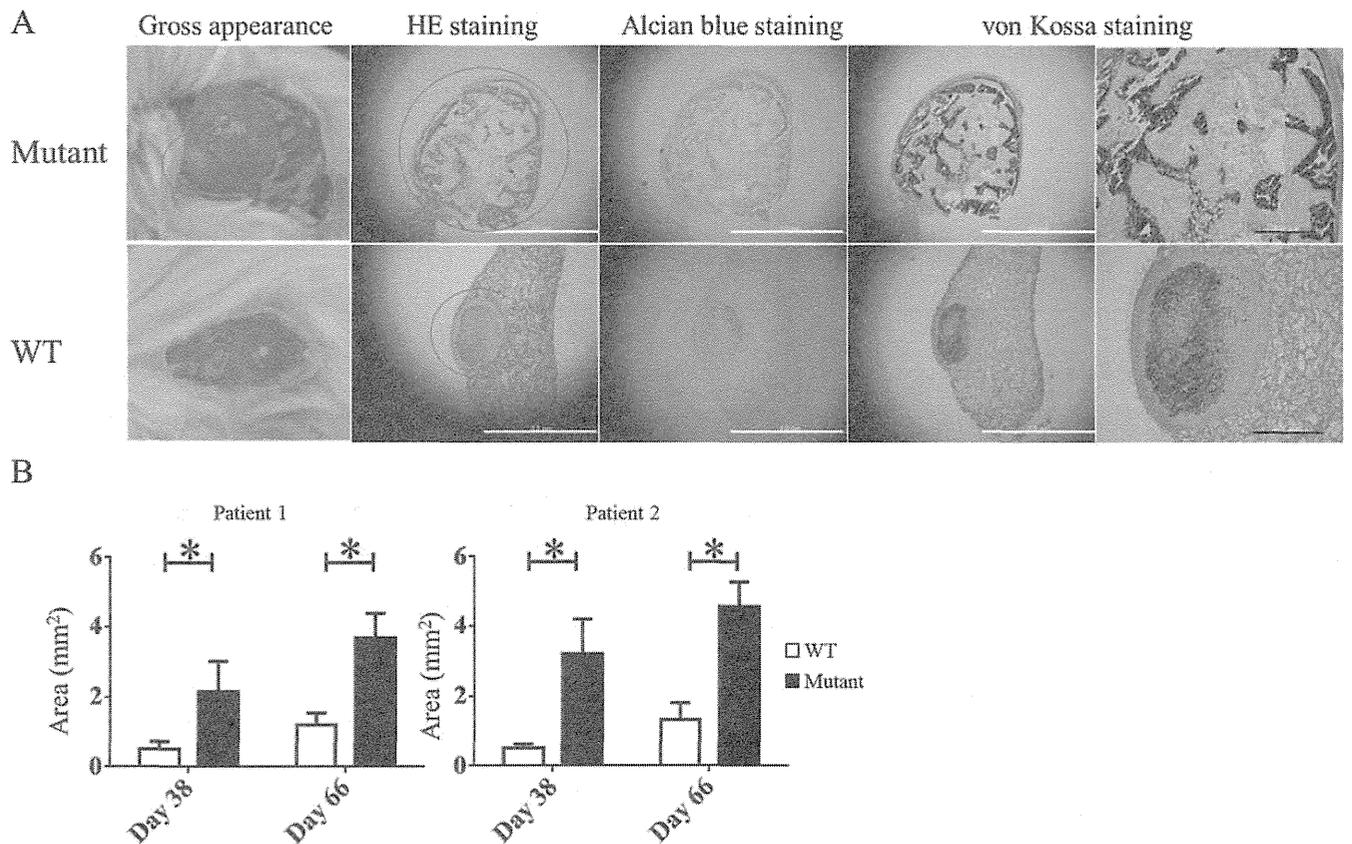
Figure 3. In vivo maturation of 3-D cell pellets derived from mutant or wild-type iPSCs from patients with neonatal-onset multisystem inflammatory disease. **A,** Images of 3-D cell pellets derived from mutant or wild-type iPSCs following transplantation into immunodeficient mice. Gross appearance, hematoxylin and eosin (H&E) staining, Alcian blue staining, von Kossa staining, and higher-magnification images of von Kossa staining are shown. Red circles indicate bone or cartilage pellets in gel form. White bars = 2.0 mm; black bars = 0.2 mm. Results shown were obtained using iPSCs from patient 1; similar results were obtained using iPSCs from patient 2. **B,** Quantitative analysis of the size of pellets when they were transplanted (day 38) and harvested (day 66). Bars show the mean ± SEM of 3 independent clones, from which duplicate measurements were obtained. Data are representative of 3 independent experiments. $*$ = $P < 0.05$. See Figure 1 for other definitions.

with abnormal ossification. The in vitro differentiation system did not induce chondrocyte calcification, probably due to the lack of cell components or factors necessary for the final differentiation step. Therefore, we used an in vivo differentiation system as a model for endochondral ossification, in which immature 3-D pellet samples were transplanted into NOG mice. The transplanted cartilage mass was vascularized in vivo (Figure 3A). Mutant pellets were larger than wild-type pellets, both at transplantation and harvesting, and this size difference increased during in vivo differentiation (Figure 3B). Following von Kossa staining, which detects calcium deposits, calcification was detected in both wild-type and mutant pellets (Figure 3A). Interestingly, Alcian blue staining revealed that mutant pellets contained more residual cartilage components than wild-

type pellets. In addition, calcified areas were scattered throughout mutant pellets, whereas they were localized in specific regions and were clearly separated from Alcian blue–positive areas in wild-type pellets. Taken together, these data indicate that in our in vivo model, chondrocyte tissue differentiated from mutant iPSCs grows larger and exhibits disorganized ossification compared to chondrocyte tissue differentiated from wild-type iPSCs.

The enhanced chondrogenesis of mutant iPSCs is independent of the NLRP3 inflammasome. The inflammatory phenotype of NOMID is caused by gain-of-function NLRP3 mutations, leading to activation of the NLRP3 inflammasome (27). Therefore, we examined the involvement of the NLRP3 inflammasome in the formation of cartilaginous masses. First, we analyzed the
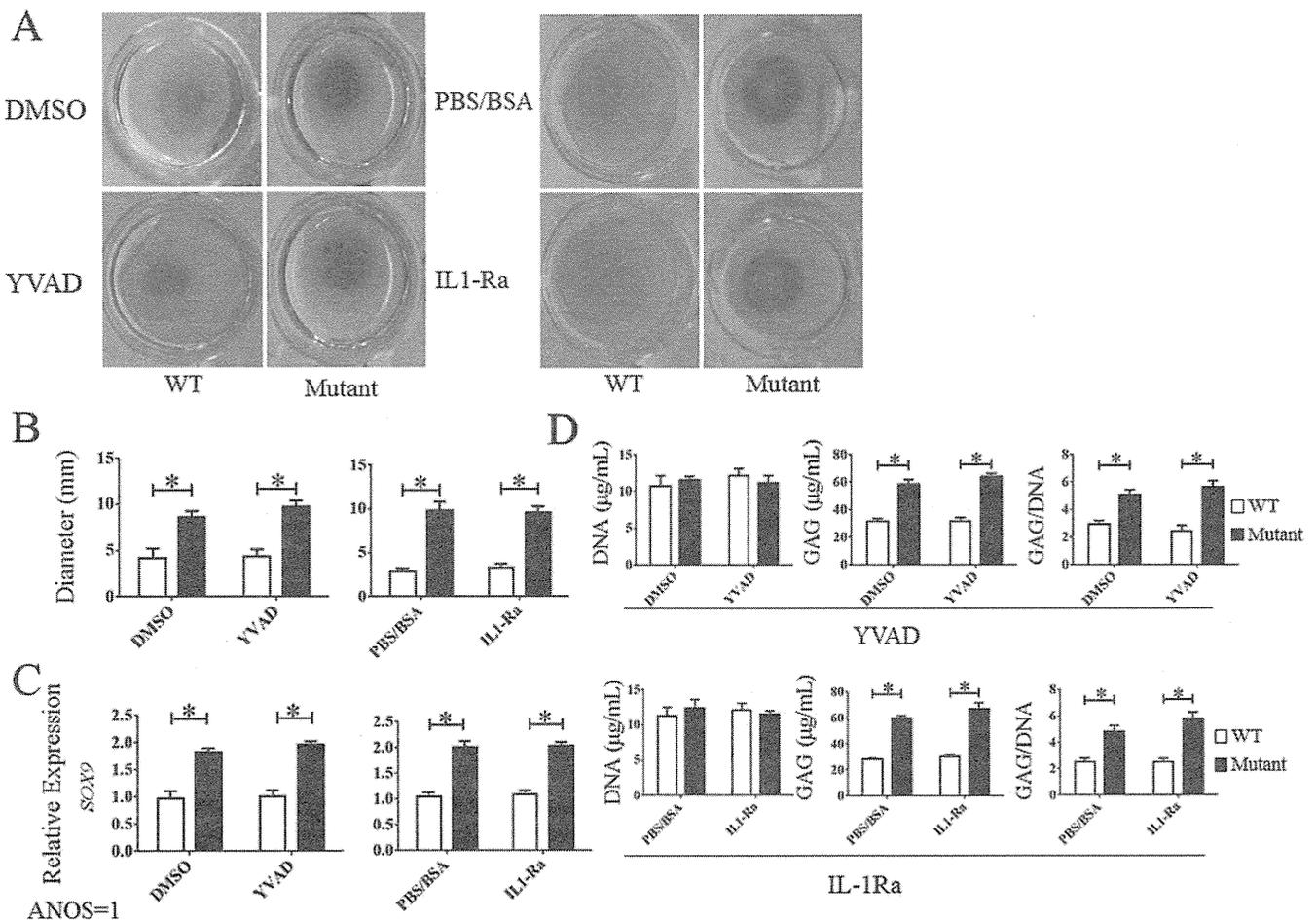
Figure 4. NLRP3 inflammasome–independent enhanced chondrogenesis of mutant iPSCs from patients with neonatal-onset multisystem inflammatory disease. Wild-type and mutant iPSCs were differentiated into chondrocytes in 2-D micromass cultures, and the caspase 1 inhibitor Ac-YVAD-CHO (YVAD; 10 μM) or human recombinant interleukin-1 receptor antagonist (IL-1Ra; 1 μg/ml) was added to the cultures. Control cultures were incubated with DMSO or phosphate buffered saline (PBS) containing bovine serum albumin (BSA). **A,** Representative 2-D micromass cultures treated with YVAD or DMSO as control (left) or with IL-1Ra or PBS/BSA as control (right). **B,** Diameter of the micromass. **C,** *SOX9* expression in chondrocytes derived from wild-type and mutant iPSCs and treated with YVAD or IL-1Ra. Expression levels are shown relative to those in ANOS cells (set at 1). **D,** DNA concentration, glycosaminoglycan (GAG) concentration, and the ratio of GAG concentration to DNA concentration in chondrocytes derived from wild-type or mutant iPSCs and treated with YVAD or IL-1Ra. Bars show the mean ± SEM of 3 independent clones from which triplicate measurements were obtained. Data are representative of 3 independent experiments. Data shown were obtained using iPSCs from patient 1; similar results were obtained using iPSCs from patient 2. $*$ = $P < 0.05$. See Figure 1 for other definitions.

expression of the NLRP3 inflammasome components in 2-D cartilage samples. Mutant and wild-type cartilage samples both expressed NLRP3, but did not express ASC, pro–caspase 1, or pro–IL-1β by Western blotting (data not shown). This suggests that the formation of large cartilaginous masses by mutant chondrocytes occurs independently of the NLRP3 inflammasome.

To confirm that chondrogenesis of mutant iPSCs is enhanced independently of the NLRP3 inflammasome, we used inhibitors of components of the

NLRP3 inflammasome, namely, Ac-YVAD-CHO, which inhibits caspase 1, and recombinant human IL-1 receptor antagonist (IL-1Ra), which antagonizes IL-1. Neither Ac-YVAD-CHO (10 μM) treatment nor recombinant human IL-1Ra (1 μg/ml) treatment during 2-D micromass culture prevented the formation of large cartilaginous masses (Figures 4A and B), *SOX9* upregulation (Figure 4C), or overproduction of GAG (Figure 4D) by chondrocytes derived from mutant iPSCs. The same was true when samples were treated
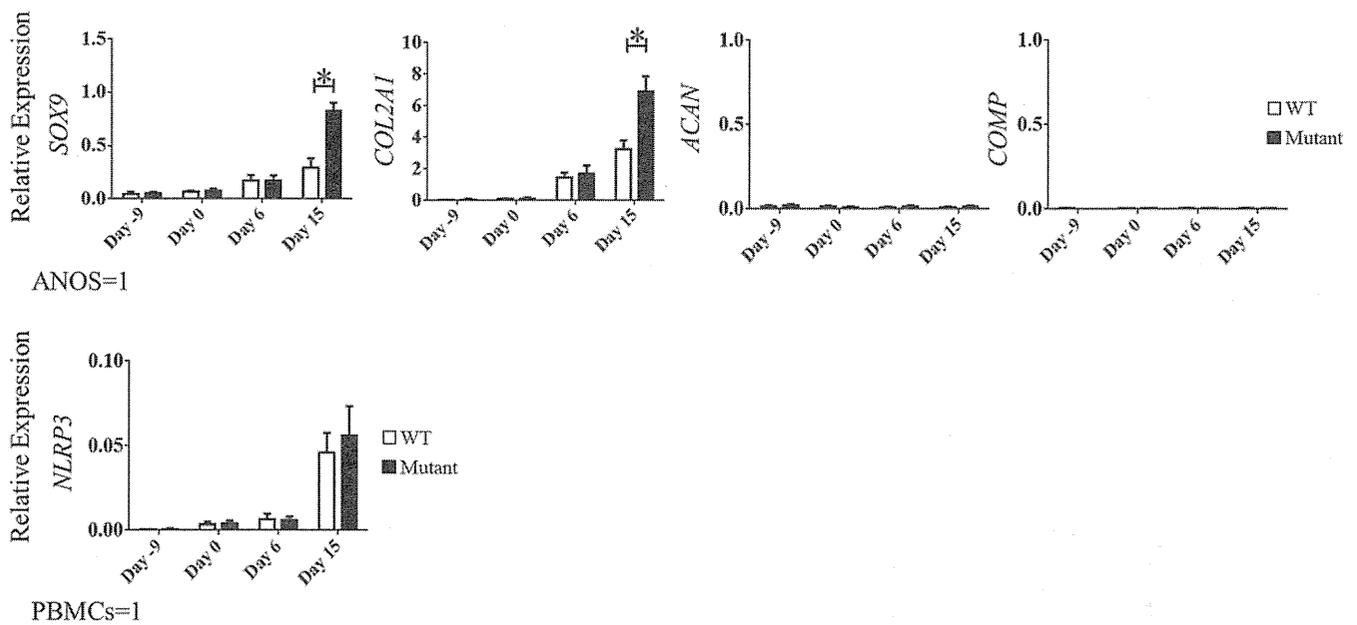
Figure 5. Up-regulation of the expression of *SOX9* and *COL2A1* in chondrocytes with mutated *NLRP3* during the chondroprogenitor cell stage. Expression of *SOX9*, *COL2A1*, *ACAN*, *COMP*, and *NLRP3* in each clone was measured in triplicate from day −9 to day 15 of chondrocyte differentiation of iPSCs from patients with neonatal-onset multisystem inflammatory disease with wild-type or mutant NLRP3. Expression levels of *SOX9*, *COL2A1*, *ACAN*, and *COMP* are shown relative to those in ANOS cells (set at 1), and the expression level of *NLRP3* is shown relative to that in peripheral blood mononuclear cells (PBMCs; set at 1). Bars show the mean ± SEM of 3 independent clones. Data are representative of 3 independent experiments with consistent results and were obtained using iPSCs from patient 1; similar results were obtained using iPSCs from patient 2. ∗ = $P < 0.05$. See Figure 1 for other definitions.

with higher concentrations of these inhibitors (up to 1,000-fold higher) (data not shown). Taken together, these data strongly indicate that the enhanced chondrogenesis of mutant iPSCs is independent of caspase 1 and IL-1, and thus the NLRP3 inflammasome.

Correlation of the up-regulation of NLRP3 with the up-regulation of SOX9 in chondroprogenitor cells. To dissect the mechanism underlying the enhanced chondrogenesis of mutant iPSCs, we analyzed the time course of chondrocyte-specific gene expression in chondroprogenitor cells (Figure 5). Expression of *SOX9*, *COL2A1*, and *NLRP3* started to be up-regulated in chondroprogenitor cells on day 6. Importantly, on day 15, *SOX9* and *COL2A1* were up-regulated more in mutant chondroprogenitor cells than in wild-type chondroprogenitor cells, whereas *NLRP3* was up-regulated similarly in both types of cells (Figure 5). In contrast, at this time point, the other chondrocyte-specific markers *ACAN* and *COMP* were not expressed in either type of cell (Figure 5). Thus, differential up-regulation of *SOX9* in chondroprogenitor cells correlated with the up-regulation of *NLRP3* and preceded the up-regulation of *COMP* and *ACAN*.

Critical role of the CREB/ATF-binding site of the SOX9 promoter in mutated NLRP3–dependent enhancement of SOX9 expression. Next, we focused on *SOX9* because it was up-regulated together with *NLRP3*, and this preceded the up-regulation of other chondrocyte-specific markers. We analyzed the activity of the human *SOX9* promoter in chondroprogenitor cells in which the level of *SOX9* mRNA was increased. We created a luciferase reporter construct containing the 5′-UTR of human *SOX9*, which encompasses −927 to +84 bp of the transcription start site. This fragment has basal promoter activity and putative binding sites for 5 transcription factors, namely, NF-AT, activator protein 1 (AP-1), NF-κB, Sp1, and CREB/ATF (see Supplementary Figure 1, available on the *Arthritis & Rheumatology* web site at http://onlinelibrary.wiley.com/doi/10.1002/art.38912/abstract). This fragment showed no promoter activity in the monocytic cell line THP-1 or the erythroleukemic cell line K562, which do not express endogenous *SOX9* (data not shown). Importantly, human *SOX9* promoter activity was higher in mutant chondroprogenitor cells than in wild-type chondroprogenitor cells (Figure 6A). To identify the element of the human *SOX9*
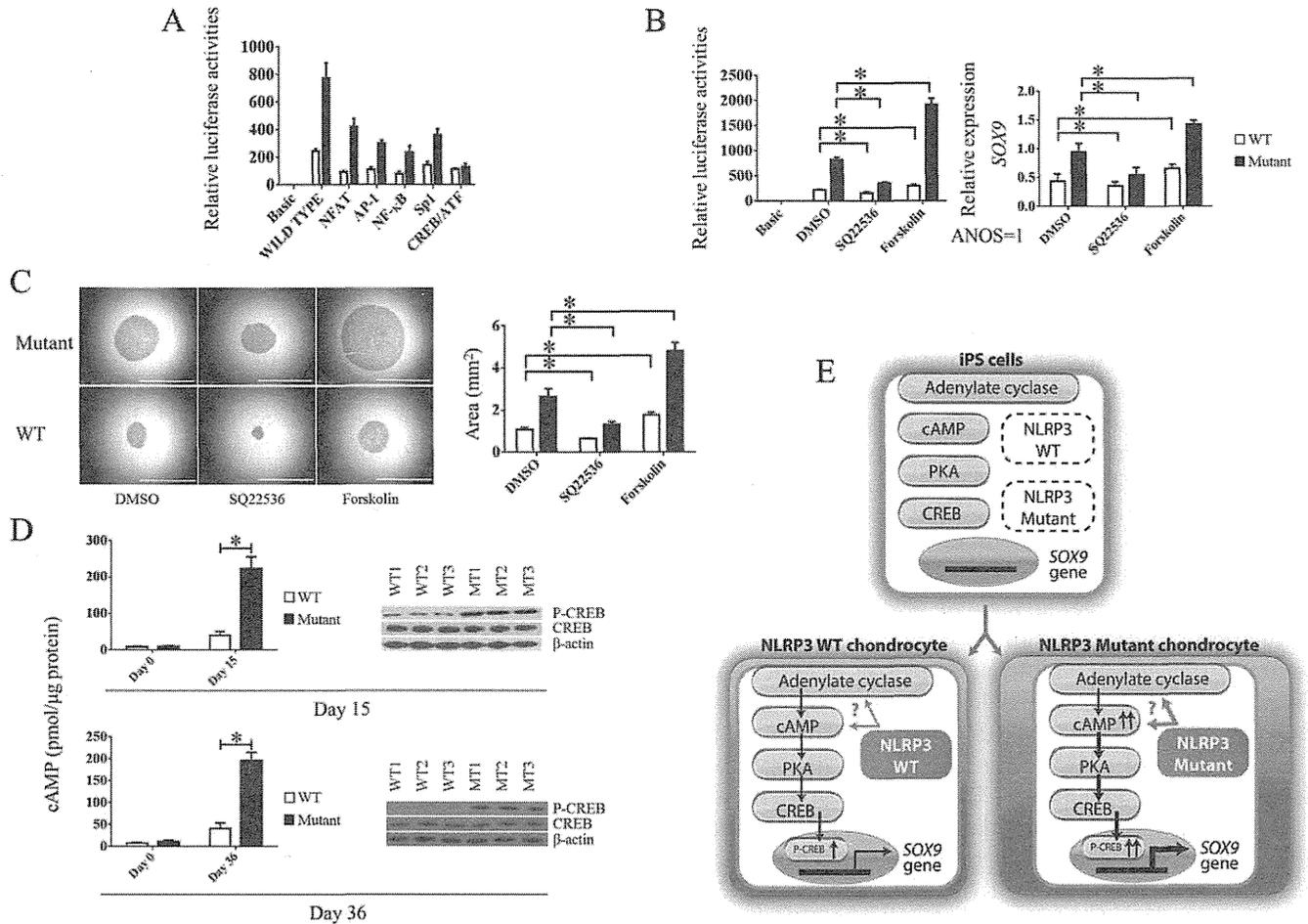
Figure 6. *SOX9* up-regulation in chondrocytes derived from iPSCs from patients with neonatal-onset multisystem inflammatory disease with mutant NLRP3 is dependent on the cAMP/protein kinase A (PKA)/CREB pathway. **A**, *SOX9* promoter activity in wild-type and mutant chondroprogenitor cells after the introduction of mutations into its transcription factor binding sites. **B**, *SOX9* promoter activity and expression in wild-type and mutant chondroprogenitor cells treated with SQ22536 or forskolin. **C**, Effects of SQ22536 and forskolin on 3-D pellets of mutant and wild-type cells. Both reagents were used at a concentration of 10 μM. Bars = 2.0 mm. **D**, Increased activity of the cAMP/PKA/CREB pathway in mutant chondroprogenitor cells compared to wild-type chondroprogenitor cells, as demonstrated by cAMP concentration in wild-type and mutant iPSCs (day 0) and chondroprogenitor cells (day 15 and day 36), and Western blot analysis of phosphorylated CREB in wild-type (WT1–3) and mutant (MT1–3) chondroprogenitor cells. **E**, Schematic diagram summarizing the molecular mechanism elucidated in this study. Bars in **A–D** show the mean ± SEM of 3 independent clones from which triplicate (**A, B**, and **D**) or duplicate (**C**) measurements were obtained. Data are representative of 2 independent experiments with consistent results and were obtained using iPSCs from patient 1; similar results were obtained using iPSCs from patient 2. ∗ = $P < 0.05$. See Figure 1 for other definitions.

promoter region that responds in a mutated NLRP3–dependent manner, we performed site-directed mutagenesis of the sites of this promoter that bind the transcription factors NF-AT, AP-1, NF-κB, Sp1, and CREB/ATF (Supplementary Figure 1). Among the reporters with these mutations, the reporter that harbored a mutation in the CREB/ATF-binding site showed the least up-regulation of *SOX9* promoter activity in mutant cells (Figure 6A and Supplementary Figure 1). Thus, we speculate that the CREB/ATF-binding site is critical for

activation of the human *SOX9* promoter in a mutated NLRP3–dependent manner.

Critical role of the cAMP/PKA/CREB pathway in SOX9 up-regulation caused by mutated NLRP3. To further explore the association between mutated NLRP3 and the cAMP/PKA/CREB pathway, we examined the effect of an adenylate cyclase activator and inhibitor (forskolin and SQ22536, respectively) on the activity of the human *SOX9* promoter and *SOX9* mRNA expression (Figure 6B). Among mutant chondroprogenitor